



 Cite this: *Med. Chem. Commun.*,  
2017, 8, 1307

# 5-Methyl-*N*-(8-(5,6,7,8-tetrahydroacridin-9-ylamino)octyl)-5*H*-indolo[2,3-*b*]quinolin-11-amine: a highly potent human cholinesterase inhibitor†‡

 Li Wang,<sup>a</sup> Ignacio Moraleda,<sup>b</sup> Isabel Iriepa,<sup>b</sup> Alejandro Romero,<sup>c</sup>  
Francisco López-Muñoz,<sup>de</sup> Mourad Chioua,<sup>f</sup> Tsutomu Inokuchi,<sup>\*a</sup>  
Manuela Bartolini<sup>\*g</sup> and José Marco-Contelles \*<sup>f</sup>

The synthesis, cholinesterase inhibition, molecular modelling and ADME properties of novel tacrine-neocryptolepine heterodimers are described. Compound **3** [5-methyl-*N*-(8-(5,6,7,8-tetrahydroacridin-9-ylamino)octyl)-5*H*-indolo[2,3-*b*]quinolin-11-amine], showing a moderate inhibition of the Aβ<sub>1-42</sub> self-aggregation (26.5% at a 1:5 ratio with Aβ<sub>1-42</sub>), and a calculated log BB value (0.27) indicating excellent potential BBB penetration, is a highly potent human cholinesterase inhibitor [IC<sub>50</sub> (hAChE) = 0.95 ± 0.04 nM; IC<sub>50</sub> (hBuChE) = 2.29 ± 0.14 nM] which can be listed among the most potent hAChE inhibitors so far identified, and is not hepatotoxic *in vitro* at the concentrations at which the ChEs are inhibited. A molecular modeling study was also undertaken in order to elucidate the AChE and the BuChE bind modes of all the new compounds. The docking results show that all of them bind to AChE in extended conformations and to BuChE in folded conformations. Moreover, these studies revealed that the length of the linker is crucial to binding both the catalytic anionic site and the peripheral anionic site.

 Received 21st March 2017,  
Accepted 26th April 2017

DOI: 10.1039/c7md00143f

rsc.li/medchemcomm

## 1. Introduction

In previous communications, some of us have reported a novel series of neocryptolepine derivatives showing potent antiplasmodial activities,<sup>1,2</sup> as well as the identification of new multi-target compounds<sup>3</sup> derived from tacrine for the potential treatment of Alzheimer's disease (AD).<sup>4</sup>

AD is a progressive neurodegenerative disease causing memory loss, disorientation, speech failure and behavioral

changes,<sup>5,6</sup> and consequently, a significant burden to public health systems worldwide.<sup>7</sup> AD is associated with pathological changes such as amyloid β-protein (Aβ) production and its aggregation as senile plaques, formation of neurofibrillary tangles composed of phosphorylated τ-protein and inflammation.<sup>8</sup> The disease is also characterized by cholinergic neuronal loss in the cerebral cortex occurring in the early stages of AD, which is correlated with impairment of cognitive functions.<sup>9</sup> Changes in other neurochemicals such as *N*-methyl-D-aspartate (NMDA) were also identified.<sup>10</sup>

Acetylcholinesterase (AChE) and butyrylcholinesterase (BuChE) enzymes are both responsible for the hydrolysis of acetylcholine (ACh) in the brain and, up to 2003, inhibitors of such enzymes have been the only therapeutic option available to treat AD. In 2003 the approval of the NMDA receptor antagonist memantine by the US FDA expanded the therapeutic options.<sup>11</sup> The development of cholinesterase inhibitors (ChEIs) as anti-AD drugs is based on the so-called "cholinergic hypothesis", which relates the impairment of the cognitive function to the progressive and massive decline of the cholinergic transmission in brain areas of AD patients.<sup>12</sup> In this light, the inhibition of cholinesterase enzymes (ChEs) should restore the normal level of ACh in cortical synapses and lead to the improvement of memory functions. Although AChE and BuChE seem to have different prevalent roles along the different stages of the pathology, both ChEs are thought to play a central role in the hydrolysis of brain ACh, thus dual

<sup>a</sup> Division of Chemistry and Biotechnology, Graduate School of Natural Science and Technology, Okayama University, 3.1.1 Tsushima-Naka, Kita-ku, Okayama 700-8530, Japan. E-mail: inokuchi@cc.okayama-u.ac.jp; Tel: +81 86 294 5045

<sup>b</sup> Departamento de Química Orgánica y Química Inorgánica, Universidad de Alcalá, Ctra. Madrid-Barcelona, Km. 33,6, 28871, Alcalá de Henares, Madrid, Spain

<sup>c</sup> Departamento de Toxicología y Farmacología, Facultad de Veterinaria, Universidad Complutense de Madrid, 28040-Madrid, Spain

<sup>d</sup> Faculty of Health, Camilo José Cela University, C/Castillo de Alarcón, 49; 28692 Villanueva de la Cañada, Madrid, Spain

<sup>e</sup> Neuropsychopharmacology Unit, "Hospital 12 de Octubre" Research Institute, Av. de Córdoba s/n, 28041 Madrid, Spain

<sup>f</sup> Laboratory of Medicinal Chemistry (IQOG, CSIC), C/ Juan de la Cierva 3, 28006-Madrid, Spain. E-mail: iqoc21@iqog.csic.es; Tel: +34 91 5622900

<sup>g</sup> Department of Pharmacy and Biotechnology, Alma Mater Studiorum, University of Bologna, Via Belmeloro 6, 40126 Bologna, Italy.

E-mail: manuela.bartolini3@unibo.it; Tel: +39 0512099729

† The authors declare no competing interests.

‡ Electronic supplementary information (ESI) available: All the experimental details. See DOI: 10.1039/c7md00143f

inhibition seems to be more beneficial for AD patients.<sup>13</sup> Currently there are four AChEIs [tacrine, (Fig. 1), galanthamine, donepezil and rivastigmine] for AD clinical treatment.<sup>14</sup>

The discovery of tacrine signaled a breakthrough in the long-term treatment of AD associated cognitive function disorders. Tacrine-HCl was the first drug approved by the US FDA in 1993 for the palliative treatment of AD. Tacrine acts as a reversible inhibitor partly competitive with the substrate.<sup>15</sup> However, the use of tacrine is limited because of the significant hepatotoxicity and cardiovascular system impairment, in spite of its mild cognitive benefits, which do not alter the course of the disease.<sup>16</sup> Therefore, the search for new tacrine analogues is still of interest for scientists involved in AD research.<sup>17</sup>

On the other hand, neocryptolepine (Fig. 1) is a minor alkaloid isolated from the roots of the West African plant *Cryptolepis sanguinolenta*,<sup>18</sup> bearing a tetracyclic heteroaromatic linearly fused indoloquinoline, and exhibiting promising antiparasitodal activity against both chloroquinesensitive and chloroquine-resistant *P. falciparum*.<sup>19</sup>

For the design of new AChEIs, the so-called “bivalent ligand strategy” has been of particular interest, mainly due to the peculiar architecture of the enzyme, with the catalytic active site (CAS) and the peripheral active site (PAS) located at the bottom and top of a gorge, respectively.<sup>20,21</sup> In the first reported example, for instance, two tacrine units were linked by a seven methylene spacer to bind both the CAS and PAS, resulting in the bivalent AChEI bis(7)-tacrine (Fig. 2), which showed enhanced affinity toward AChE compared to tacrine.<sup>22</sup>

## 2. Results and discussion

### 2.1. Design of the novel tacrine–neocryptolepine heterodimers

In this context, and in the search for potent tacrine analogues endowed with lower or absent hepatotoxicity,<sup>23</sup> we have designed new tacrine–neocryptolepine heterodimers (**I**) (Fig. 1) for the potential treatment of AD, with the expectation that the tacrine motif should bind to the CAS, and the fully planar aromatic neocryptolepine motif might establish easy and appropriate interaction at the PAS of AChE, resulting in more potent AChEIs than tacrine. Thus, we have synthesized compounds **1–3** (Fig. 1), three members of the family of compounds of type **I**, by modifying the length of the spacer from 4 to 6 and 8 methylene units, and investigated their ChE inhibitory profile. As a result, we have identified compound **3** [5-methyl-*N*-(8-(5,6,7,8-tetrahydroacridin-9-ylamino)octyl)-5*H*-indolo[2,3-*b*]quinolin-11-amine] as a highly potent human ChEI (hChEI), which can be listed among the most potent hAChE inhibitors so far identified.

### 2.2. Synthesis of the novel tacrine–neocryptolepine heterodimers

The synthesis of the new compounds **1–3** has been easily achieved by coupling commercial 1,*n*-diamines **4**,<sup>24</sup> **5**,<sup>25</sup> and **6**,<sup>25</sup> with 11-chloro-5-methyl-5*H*-indolo[2,3-*b*]quinolone (**7**),<sup>26</sup> in good yield and under standard reaction conditions (ESI†).

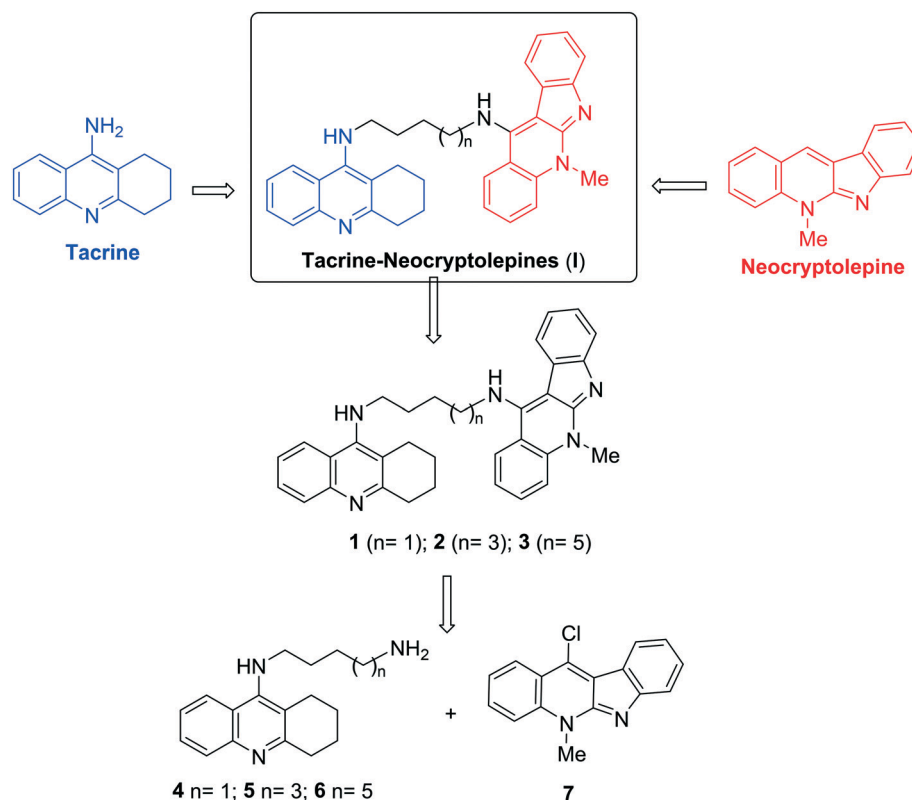


Fig. 1 General structure of neocryptolepine, tacrine, the new tacrine–neocryptolepines (**I**), and the heterodimers **1–3** described in this work.

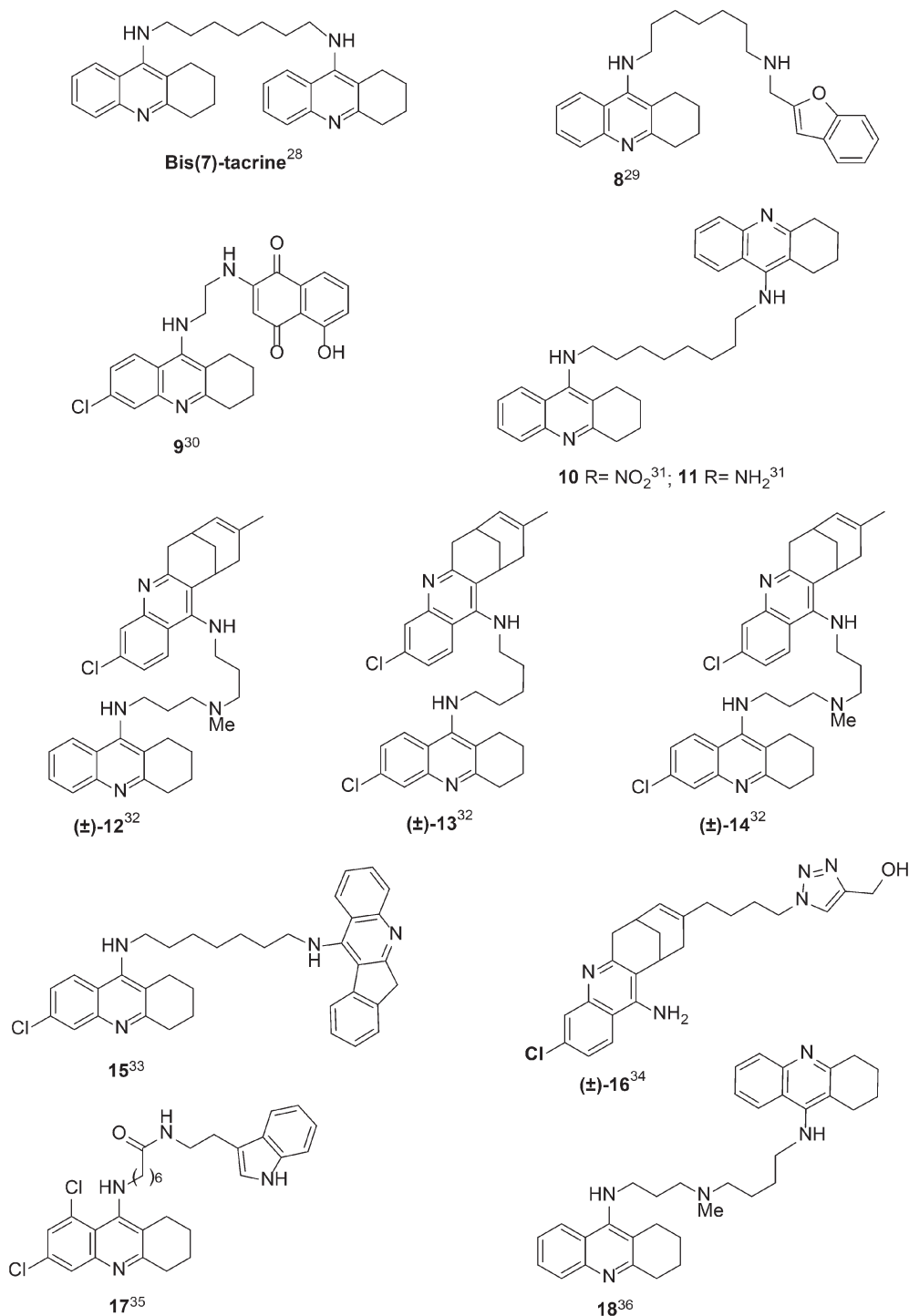


Fig. 2 Structure of bis(7)tacrine and other highly potent tacrine-heterodimers 8–18.

All new compounds showed analytical and spectroscopic data in good agreement with their structures.

### 2.3. Biological characterization of the novel tacrine–neocryptolepine heterodimers

The new tacrine–neocryptolepine derivatives were evaluated as inhibitors of human AChE (hAChE) and human BuChE

(hBuChE) following the method of Ellman.<sup>27</sup> As shown in Table 1, compounds 1–3 are very potent hAChEIs, with IC<sub>50</sub> values in the nanomolar range, showing low to moderate selectivity *versus* hBuChE. The most potent hAChEI was hybrid 3 ( $n = 5$ ) [IC<sub>50</sub> = 0.95 ± 0.04 nM], which is 1.31-fold more potent than hybrid 2 ( $n = 3$ ), and 55.7-fold more potent than hybrid 1 ( $n = 0$ ). This trend clearly shows that the inhibitory potency towards hAChE increases with the length of the linker.

**Table 1** Inhibition of hAChE and hBuChE by tacrine–neocryptolepines 1–3, tacrine, bis(7)tacrine, and highly potent tacrine heterodimers 8–18 available from the literature

Compound	hAChE (IC <sub>50</sub> , nM) <sup>a</sup>	hBuChE (IC <sub>50</sub> , nM) <sup>a</sup>	hAChE selectivity <sup>b</sup>	Aβ <sub>1–42</sub> self-aggregation (% inhibition) <sup>c</sup>
1	53.0 ± 2.7	21.8 ± 1.3	0.41	19.7 ± 1.5
2	1.25 ± 0.12	9.00 ± 0.43	7.20	25.9 ± 2.4
3	0.95 ± 0.04	2.29 ± 0.14	2.41	26.5 ± 4.2
Tacrine	350 ± 10	40 ± 2	0.11	<5
Bis(7)tacrine <sup>28</sup>	0.81 ± 0.09	5.66 ± 0.15	0.14	53.4 ± 1.4
8 <sup>29</sup>	0.86 ± 0.05	2.18 ± 0.15	0.4	61.3 ± 4.5
9 <sup>30</sup>	0.72 ± 0.06	542 ± 16	753	37.5 ± 4.9
10 <sup>31</sup>	0.78 (Ki)	0.06 (Ki)	13	nd
11 <sup>31</sup>	0.23 (Ki)	8.26 (Ki)	0.028	nd
(±)-12 <sup>32</sup>	0.42 ± 0.04	139 ± 5.2	331	28.1 ± 6.4
(±)-13 <sup>32</sup>	0.74 ± 0.0	75.2 ± 2.6	102	30.9 ± 2.2
(±)-14 <sup>32</sup>	0.31 ± 0.02	51.3 ± 4.6	165	51.3 ± 4.6
15 <sup>33</sup>	1.05 ± 0.08	63.7 ± 3.5	60.7	nd
16 <sup>34</sup>	0.43 ± 0.04	210 ± 20	488	nd
17 <sup>35</sup>	0.008 ± 0.0004	7.8 ± 0.4	975	nd
18 <sup>36</sup>	0.012 (Ki)	0.82 (Ki)	0.01	nd

<sup>a</sup> Each IC<sub>50</sub> value is the mean ± SEM of at least two independent experiments in which each point was determined in duplicate/triplicate.

<sup>b</sup> Selectivity for hAChE = IC<sub>50</sub> (hBuChE)/IC<sub>50</sub> (hAChE). <sup>c</sup> Percent inhibition with inhibitor at 10 μM (5 : 1 [Aβ<sub>42</sub>] : [I]).

Regarding the inhibition of hBuChE, the most potent hBuChEI was again compound 3 [IC<sub>50</sub> = 2.29 ± 0.14 nM], being 3.91 and 9.51-fold more potent than analogues 2 and 1, respectively. As shown, the same trend applies for the inhibition of hBuChE: the longer the linker, the stronger the inhibitory potency. Regarding the hAChE/hBuChE selectivity, the selectivity ratio decreases from 7.2 to 2.41 and 0.41, for hybrids 2, 3, and 1, respectively. Thus, compound 2 is the hybrid endowed with the higher hAChE selectivity. As shown in Table 1, compound 3 is much more potent than tacrine<sup>28</sup> for the inhibition of both ChEs: 368.4- and 17.4-fold for hAChE and hBuChE, respectively, and equipotent to bis(7)tacrine<sup>28</sup> (Fig. 2) for both ChEs.

The results claimed here for hybrid 3 confirm that this compound is a highly potent hAChEI and stands among the most potent tacrine-heterodimers (Fig. 2) so far developed, which mostly (compounds 8–16) showed inhibitory potencies in the high sub-nanomolar range (0.23–1.05 nM)<sup>29–36</sup> (Fig. 2). To the best of our knowledge, only two derivatives showed significantly higher (about two orders of magnitude) potency, namely, derivative 7-(6,8-dichloro-1,2,3,4-tetrahydro-acridin-9-ylamino)-heptanoic acid [2-(1*H*-indol-3-yl)-ethyl]-amide (17) (Fig. 2), a recently described tacrine–melatonin hybrid,<sup>35</sup> which is 118.7-fold more potent hAChEI, but conversely, 3,4-fold less potent hBuChEI than our tacrine analogue 3, and the analogue of bis(7)tacrine 18<sup>36</sup> (Fig. 2) bearing an NMe group in the tether between the two tacrine fragments as a midgorge recognition site. This compound showed a balanced inhibitory potency in the picomolar range towards both ChEs (Ki is equal to 0.012 and 0.82 nM for hAChE and hBuChE, respectively).

In order to explain the observed binding affinities, docking analysis has been carried out with compounds 1–3 on hAChE.

## 2.4. Molecular modeling studies

The blind docking technique was used for the detection of possible binding sites and modes of peptide ligands, by scanning the entire surface of protein targets, so that a location with the highest binding affinity on the proteins may be found. Docking simulations were carried out using AutoDock Vina.<sup>37</sup> The crystal structures of hAChE complexed with fasciculin-II and hBuChE bound with tacrine were taken from RCSB Protein Data Bank (PDB ID: 1B41 and PDB ID: 4BDS).

To account for flexibility during docking, flexible torsion in the ligand was assigned, and the dihedral angles were allowed to rotate freely. The protein flexibility in docking schemes is widely accepted because it has been found that small movements in the side chain or backbone of the protein can be enough either to increase or decrease the size of the active site, or to alter the hydrogen-bonding pattern between the protein and ligand. The incorporation of protein structural flexibility into the ligand generation procedure has been commonly used in previous studies;<sup>38</sup> in particular, when the ligands are large and bulky, Trp286, Tyr124, Tyr337 and Tyr72, Asp74, Thr75, Trp86, and Tyr341 receptor residues have been selected to be flexible during docking simulation. These eight residues delineate the shape of the gorge entry and lining of the AChE, as their motion may significantly enlarge the gorge mouth to facilitate ligand access to the catalytic site.

Compounds 1–3, bearing indoloquinoline and tacrine moieties connected with a polymethylene bridge with two nitrogen atoms, showed a significant increase of potency with the elongation of the linker.

Visual inspection of the top scored pose of 1 reveals that the ligand is accommodated at the active-site gorge (Fig. 3). In this position, compound 1 only established a series of contacts with the amino acid residues at the PAS and mid-gorge, but could not reach the CAS due to the length of the linker.

In particular, it interacts at the PAS *via* a bifurcated hydrogen bond with Thr75 and with Val73 by its NH group. In addition, the other NH group forms a hydrogen bond with the mid-gorge site Asp74 (Fig. 4).

Compound 2 exhibited dual binding site mode of interaction, with a distally lodged indoloquinoline core at the PAS of the hAChE, while the tacrine moiety is oriented towards the CAS region of the enzyme (Fig. 5). In more detail, the indoloquinoline moiety is sandwiched by  $\pi$ - $\pi$  interactions between Trp286 and Tyr341. The phenyl ring of the indole is engaged in anion- $\pi$  interactions with Asp74. Several aromatic residues (Phe297, Tyr337, Phe338) delineated the tether between the two pharmacophores contributing to ligand accommodation by hydrophobic interactions. The amino group shows hydrogen bonds with Asp74 and Tyr124, thus enhancing the ligand-enzyme interaction in the PAS. At the bottom of the gorge, the tacrine moiety exhibited favourable parallel  $\pi$ - $\pi$  interactions with Tyr337 and Trp86; it was placed in the vicinity of His447 (catalytic triad residue) and van der Waals interactions were established (Fig. 6).

Finally, compound 3 is bound to the hAChE active site in a similar fashion as 2. This involves orientation of the indoloquinoline unit into the PAS region while the tacrine moiety is oriented towards the CAS region of the enzyme. The indoloquinoline moiety facilitates  $\pi$ - $\pi$  stacking with the side chain of Trp286 from the PAS at the gorge opening (Fig. 7). Similarly, the tacrine motif at the opposite terminal enables  $\pi$ - $\pi$

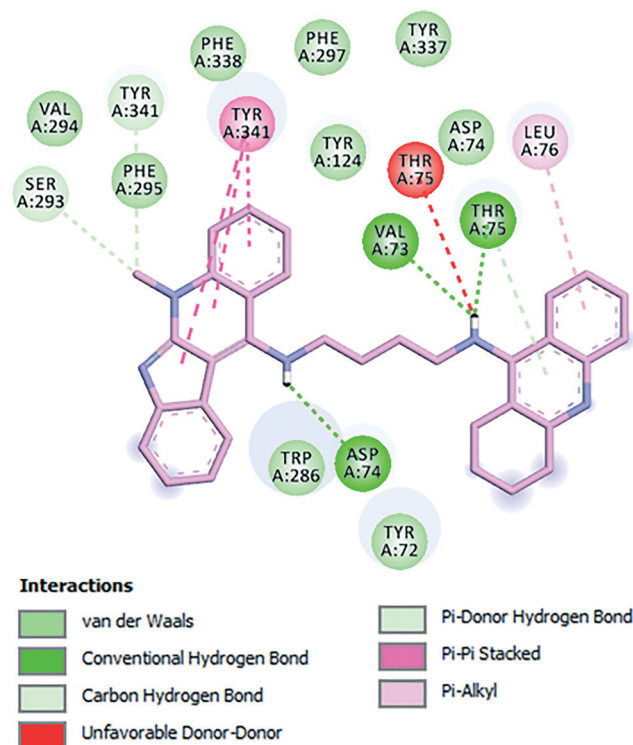


Fig. 4 Schematic representation of different interactions of compound 1 with hAChE.

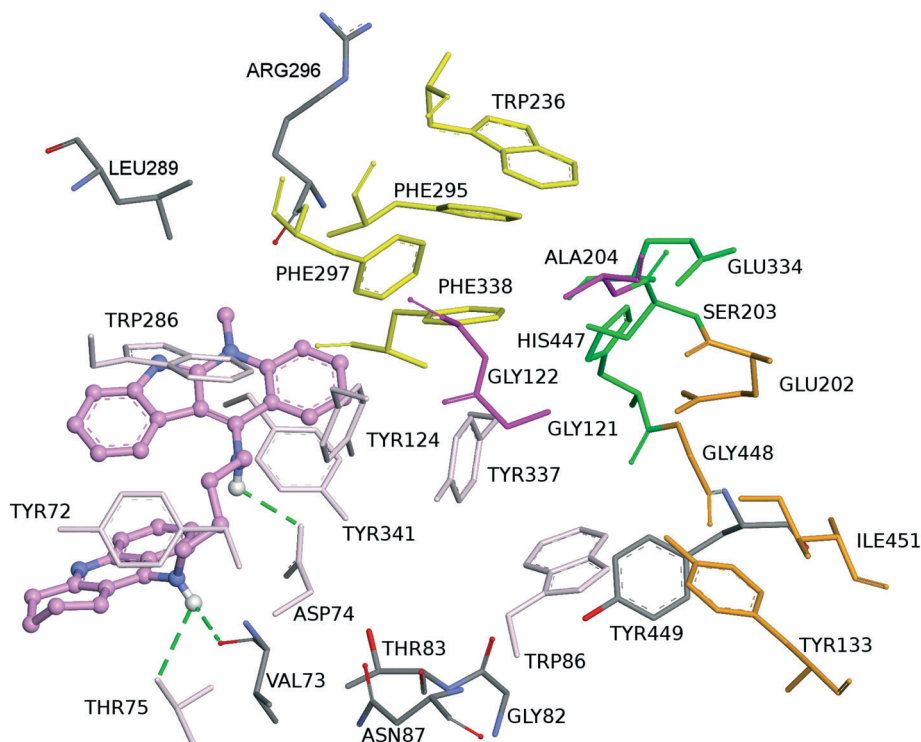
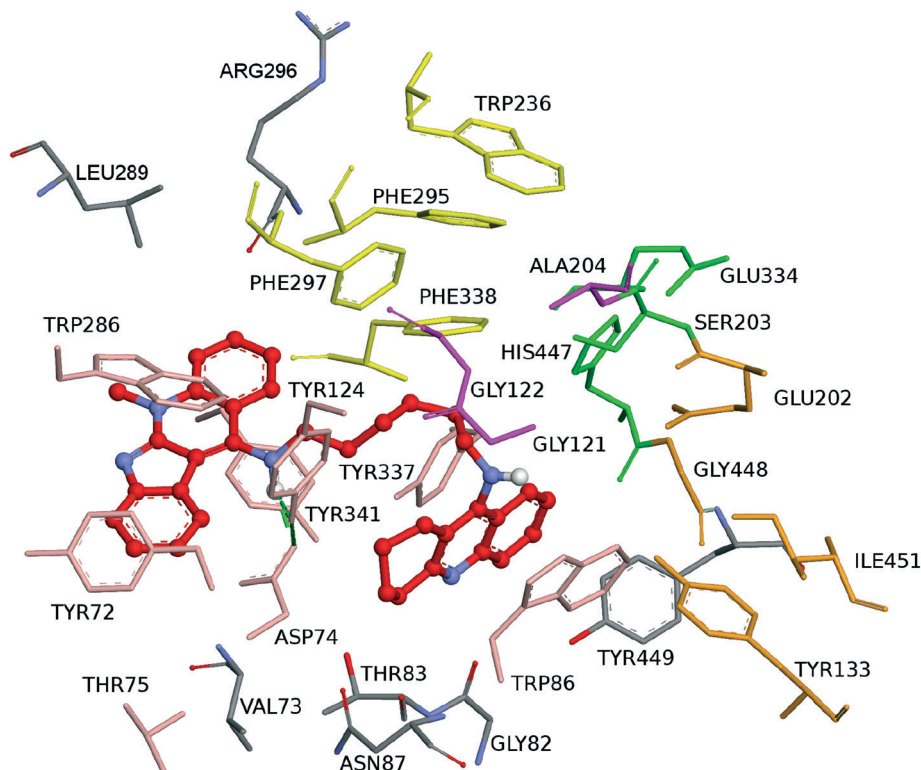


Fig. 3 Binding mode of inhibitor 1 at the active site of hAChE. Compound 1 is illustrated in violet. The ligand is rendered as balls and sticks and the side chain conformations of the mobile residues are illustrated in the same color as the ligand. Different subsites of the active site were colored: catalytic triad (CT) in green, oxyanion hole (OH) in magenta, anionic sub-site (AS) in orange, except Trp86, acyl binding pocket (ABP) in yellow, and peripheral anionic subsite (PAS) in light pink. Dashed green lines are drawn among atoms involved in hydrogen bond interactions.





**Fig. 5** Binding mode of inhibitor 2 at the active site of hAChE. Compound 2 is illustrated in red. The ligand is rendered as balls and sticks and the side chain conformations of the mobile residues are illustrated in the same color as the ligand. Different subsites of the active site were colored: catalytic triad (CT) in green, oxyanion hole (OH) in magenta, anionic sub-site (AS) in orange, except Trp86, acyl binding pocket (ABP) in yellow, and peripheral anionic subsite (PAS) in light red. Dashed green lines are drawn among atoms involved in hydrogen bond interactions.

interactions with Trp86 and Tyr337, which are both members of CAS; it is located in the vicinity of His447 (catalytic triad residue), establishing van der Waals interactions. Furthermore, the long aliphatic chain linking the two aromatic moieties exhibits hydrophobic contact with several aromatic residues (Tyr72, Tyr124, Trp286, Tyr337, Phe338 and Tyr341). Moreover, this chain contains several nitrogen atoms, which can act as hydrogen donors to Arg296 (Fig. 8a and b). This would tighten the binding between compound 3 and the active site gorge.

To clarify the substantial improvement in AChE binding affinity observed on going from inhibitor 1 to 3, which differ only in the length of the linker, a comparison of the binding modes of compounds 1–3 has been done (Fig. 9). Thus, it is found that the flexible octamethylene linker has the optimum length and conformational mobility to connect the peripheral and catalytic sites of AChE. Compound 2, equipped with a shorter linker, could also interact simultaneously with the PAS and the CAS of AChE. The decrease of affinity by one order of magnitude can be related to the presence of a weaker pattern of interaction with the PAS. Finally, compound 1 established a series of contacts with PAS and the mid-gorge, but could not reach the CAS due to the shorter length of the linker.<sup>39</sup>

Similar docking analysis of compounds 1–3 on hBuChE has been carried out and described in the ESI.† Interestingly, even if the binding mode of compound 1 in the hAChE active site is not very different from the binding mode in the

hBuChE active site, the orientations and conformations of compounds 2 and 3 in AChE are completely different from those in hBuChE. These ligands bind to hAChE with extended conformations whereas they bind to hBuChE with folded conformations (Fig. 7S, ESI.†). The docking calculations of compounds 1–3 at the active sites of hAChE and hBuChE can also explain the hAChE/hBuChE selectivity. All compounds bound to the hAChE with a lower binding energy compared with hBuChE. The energy gap values in hBuChE and in hAChE are in agreement with the experimentally determined selectivity (see the ESI.†).

## 2.5. ADME of tacrine–neocryptolepine derivatives 1–3

The druggability of compounds 1–3 has been investigated by calculating their absorption, distribution, metabolism and elimination (ADME) properties, using the QikProp module of Schrodinger suite (QikProp, version 3.8, Schrodinger, LLC, New York, NY, 2013).

About 45 physically significant descriptors and pharmacologically relevant properties of compounds 1–3 were predicted and some of the important properties were analyzed. All the compounds showed significant values for the properties analyzed and showed drug-like characteristics based on Lipinski's rule of five (see Table 1S, ESI.†).

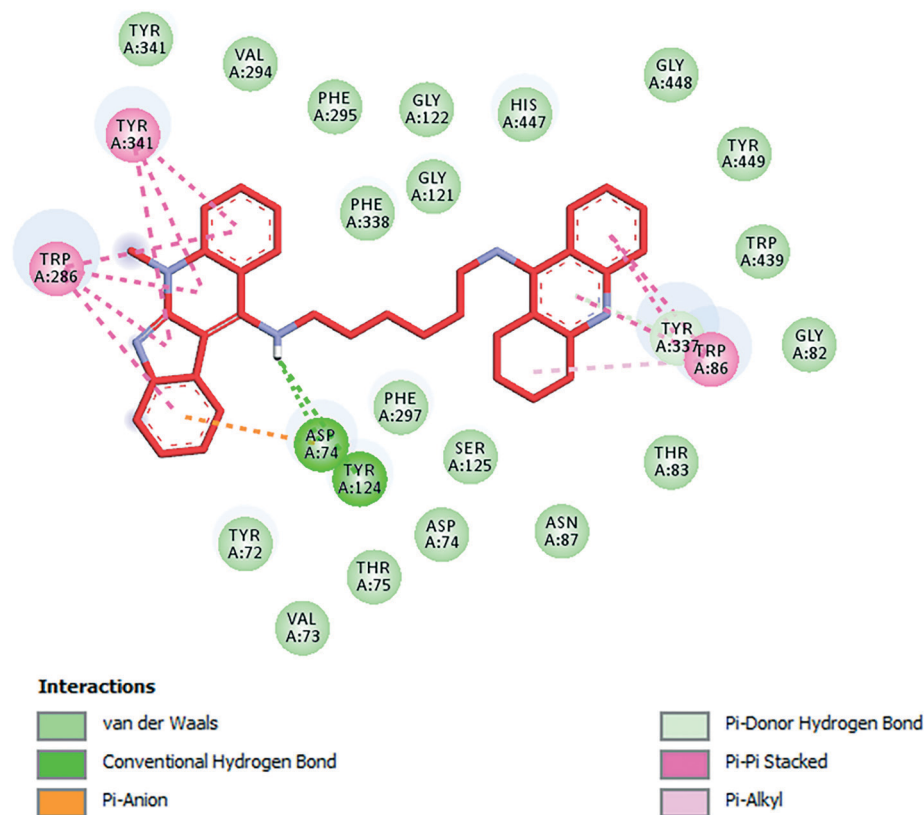


Fig. 6 Schematic representation of different interactions of compound 2 with hAChE.

First of all, factors that are relevant to the success of CNS drugs were analyzed. Usually, CNS drugs show values of MW < 450, HB donor < 3, HB acceptors < 7, QPlogPo/w < 5, PSA < 90, number of rotatable bonds < 8 and hydrogen bonds < 8. Thus, based on the value shown in Table 1S (ESI<sup>†</sup>), compounds 1–3 satisfied most characteristics of CNS acting drugs.

The solubility of organic molecules in water has a significant impact on many ADME-related properties. The three compounds showed solubility values within the limits. The partition coefficient (QPlogPo/w), which is critical for the estimation of absorption within the body, ranged between 2.42 and 3.97 (Table 1S, ESI<sup>†</sup>).

The blood brain barrier (BBB) must be crossed for the effect of compounds to be executed. Then, the hydrophilicity (logS) and logBB are the most important descriptors for CNS penetration. Experimental values of logBB cover the range from about -2.00 to +1.04. Within this range, compounds with logBB > 0.30 cross the BBB readily, while compounds with logBB < -1.00 are poorly distributed into the brain. The logBB values for compounds 1, 2 and 3 (0.55, 0.39 and 0.27, respectively) (see Table 1S, ESI<sup>†</sup>) were very close or even greater than 0.30, indicating excellent potential for BBB penetration. A literature survey suggests that polar surface area (PSA) is a measure of a molecule's hydrogen bonding capacity and its value should not exceed a certain limit if the compound is intended to be CNS active. The most active CNS drugs have PSA lower than 70 Å<sup>2</sup>. The values of PSA for compounds 1–3 are around 45 Å<sup>2</sup>, confirming good penetration

into the BBB. Similarly, the percentage human oral absorption of the compounds is in the range of 60–70% (see Table 1S, ESI<sup>†</sup>).

Other physicochemical descriptors obtained by QikProp (Table 1S, ESI<sup>†</sup>) are within the acceptable range for human use, thereby indicating their potential as drug-like molecules and a possible CNS drug.

## 2.6. Inhibition of amyloid self-aggregation

Both bis(7)tacrine<sup>40</sup> and several tacrine hybrids bearing a properly spaced aromatic fragment<sup>29,30,32,41</sup> showed significant inhibitory potency towards Aβ self-aggregation. Indeed, studies of structure activity relationships (SARs) in curcumin derivatives by Reinke and Gestwicki<sup>42</sup> clearly highlighted, among other features, the importance of having two aromatic moieties properly spaced to achieve inhibitory properties towards Aβ aggregation. Based on these premises, we hypothesized that the planar 5-methyl-5H-indolo[2,3-b]quinoline structure (neocryptolepine motif) could suitably impart anti-aggregating properties to tacrine–neocryptolepine. It is worth noting that the tetrahydroacridine scaffold of the approved drug tacrine is not able *per se* to significantly interfere with Aβ aggregation.<sup>43</sup>

Compounds 1–3 were *in vitro* evaluated for their anti-aggregating activity using a previously developed fluorescence-based assay, which enables monitoring a reproducible spontaneous self-assembly of Aβ<sub>1–42</sub> into fibrillary

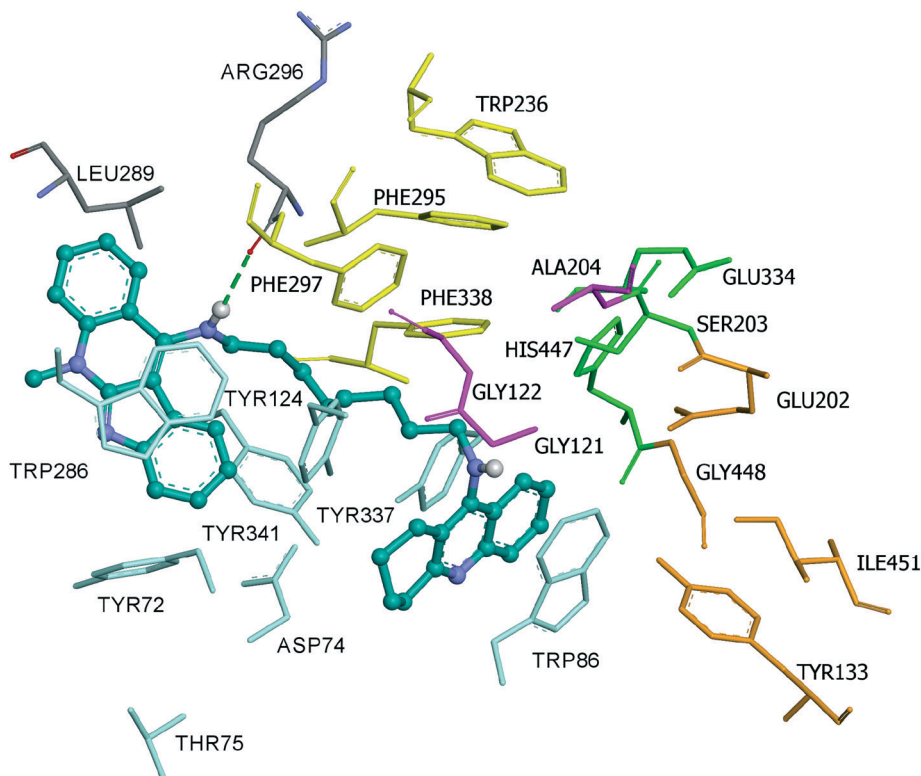


Fig. 7 Binding mode of inhibitor 3 at the active site of hAChE. Compound 3 is illustrated in turquoise. The ligand is rendered as balls and sticks and the side chain conformations of the mobile residues are illustrated in the same color as the ligand. Different subsites of the active site were colored: catalytic triad (CT) in green, oxanion hole (OH) in pink, anionic sub-site (AS) in orange, except Trp86, acyl binding pocket (ABP) in yellow, and peripheral anionic subsite (PAS) in light turquoise. Dashed green lines are drawn among atoms involved in hydrogen bond interactions.

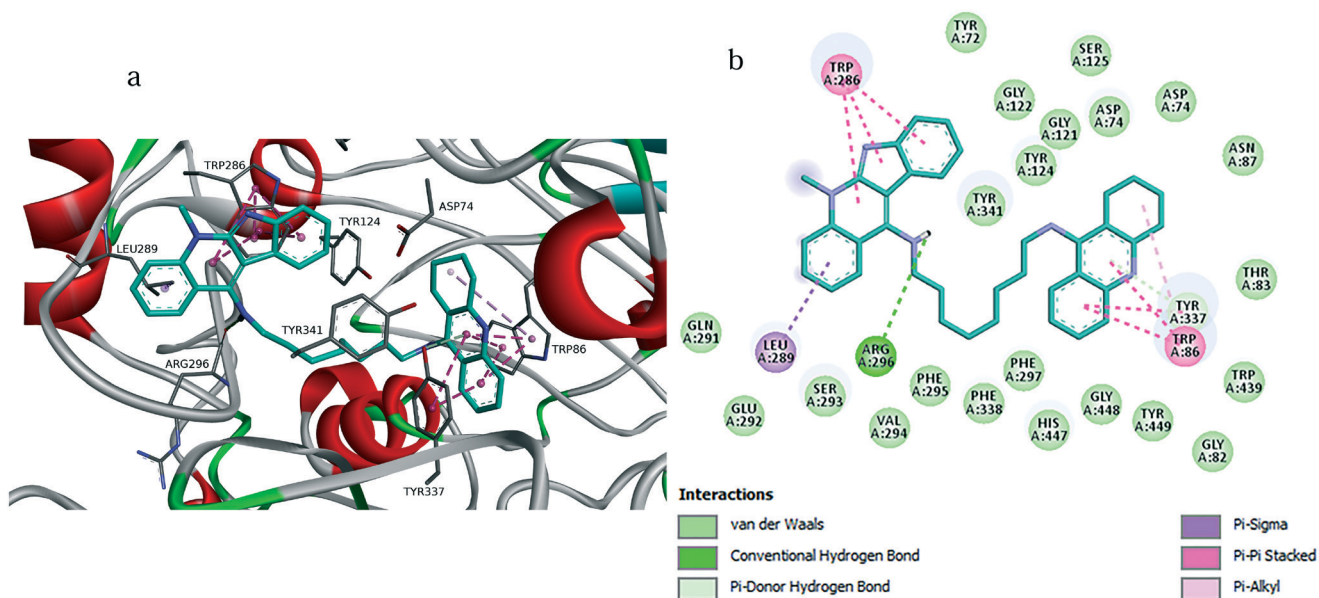
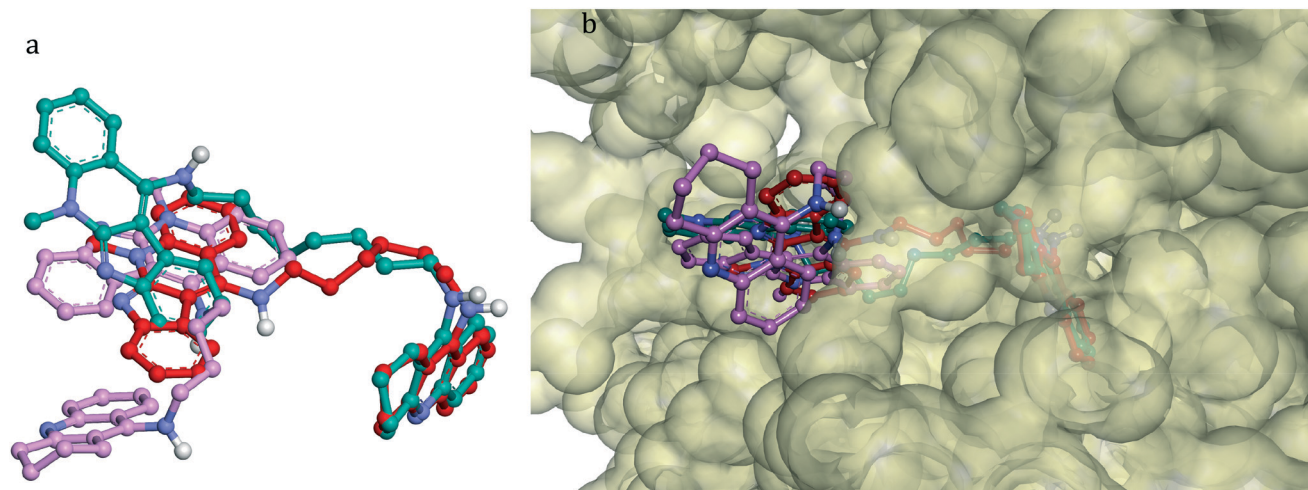


Fig. 8 a) Docking pose of compound 3 into hAChE, highlighting the protein residues that establish the main interactions with the ligand. b) Schematic representation of different interactions of compound 3 with hAChE.

structures.<sup>43</sup> Among the different peptide isoforms,  $A\beta_{1-42}$ , the 42-residue long isoform was selected on the basis of the high tendency to aggregate and accumulate in the brain leading to increased neurotoxicity.<sup>44,45</sup> Bis(7)tacrine and tacrine

were tested as positive and negative reference compounds. All the compounds and references were evaluated at 10  $\mu$ M, *i.e.* at an inhibitor/amyloid ratio of 1/5. All three tacrine-neocryptolepines were shown to significantly inhibit  $A\beta_{42}$





**Fig. 9** Superposition of the bioactive conformations for compounds 1–3 in hAChE. a) Compound 1 is rendered in a pink ball and stick model; compound 2 is rendered in a red ball and stick model; compound 3 is rendered in a turquoise ball and stick model. b) Top view of the accessible surface of the active site gorge.

self-aggregation (by 19.7–26.5%) even if at a lower extent than bis(7)tacrine (53.4%). Percent inhibition by bis(7)tacrine was in line with previously reported data.<sup>29</sup> The observed trend of inhibition suggests the influence of the length of the tether on the inhibitory activity, being higher for hybrids bearing a longer spacer chain (6–8 methylene units).

### 2.7. The hepatotoxicity of tacrine–neocryptolepines 1–3

The *in vitro* toxicity of tacrine–neocryptolepines 1–3 has been determined in HepG2 cells, at concentrations ranging from 1 to 300  $\mu\text{M}$ , and using tacrine for comparative purposes (see the ESI†).<sup>46</sup>

Conversely to what was expected, tacrine–neocryptolepines 1–3, when tested at concentrations equal to or higher than 10  $\mu\text{M}$ , showed significant toxicity which did not follow a concentration-dependent trend. At the highest tested concentration (300  $\mu\text{M}$ ), all the hybrids exerted an *in vitro* toxicity similar to that of tacrine (35–40%). However, when assayed at 1  $\mu\text{M}$ , hybrid 1 was safe with no significant alteration of cell

viability, followed by hybrid 3 which caused only a slight reduction of cell viability. Hybrid 2 was the most toxic among the three tacrine–neocryptolepines, being significantly toxic at all tested concentrations. No clear correlation between the length of the spacer chain and the toxicity toward HepG2 cells could be derived. However, considering that compounds 1 and 3 are one and two orders of magnitude more potent than tacrine as AChEI, respectively, it might be expected that the required dose is lower than that of tacrine, and thus lower is the risk for toxicity. Indeed, it is of paramount importance from the therapeutic point of view that compound 3 is not toxic *in vitro* at the concentrations at which the ChEs are inhibited Table 2.

## 3. Conclusions

In this communication we have reported the synthesis, hChE inhibition, docking analyses and prediction of ADME properties for three members of a new family of novel tacrine–neocryptolepine heterodimers, among which we have identified hybrid 3 [5-methyl-N-(8-(5,6,7,8-tetrahydroacridin-9-ylamino)-octyl)-5H-indolo[2,3-b]quinolin-11-amine] as a highly potent hChEI, and whose binding affinities as a dual inhibitor showing interaction with both the CAS and the peripheral site, have been nicely explained by molecular modelling. Furthermore, hybrid 3 was able to inhibit  $\text{A}\beta_{42}$  self-aggregation when tested at a 1/5 ratio with  $\text{A}\beta$ . These results pave the way for the design and synthesis of new related analogues aiming at reducing the hepatotoxicity and at investigating in depth other biological targets implicated in the progress and development of AD. This work is in progress and will be reported in due course.

## Acknowledgements

JMC thanks Universidad Camilo José Cela for support (Project 2014-35: NEW MULTIMOL).

**Table 2** *In vitro* toxicity of tacrine–neocryptolepines 1–3 and reference compound tacrine in HepG2 cells

Comp	1 $\mu\text{M}$	10 $\mu\text{M}$	100 $\mu\text{M}$	300 $\mu\text{M}$
1	99.5 $\pm$ 0.7 <sup>ns</sup>	37.2 $\pm$ 3.4 <sup>***</sup>	33.8 $\pm$ 3.0 <sup>***</sup>	34.8 $\pm$ 2.9 <sup>***</sup>
2	40.9 $\pm$ 0.9 <sup>***</sup>	34.9 $\pm$ 4.5 <sup>***</sup>	36.2 $\pm$ 3.7 <sup>***</sup>	36.5 $\pm$ 4.0 <sup>***</sup>
3	78.1 $\pm$ 2.3 <sup>*</sup>	41.4 $\pm$ 4.6 <sup>***</sup>	38.4 $\pm$ 3.3 <sup>***</sup>	37.9 $\pm$ 1.9 <sup>***</sup>
Tacrine	93.4 $\pm$ 4.7 <sup>ns</sup>	88.7 $\pm$ 3.4 <sup>ns</sup>	64.3 $\pm$ 4.5 <sup>***</sup>	40.0 $\pm$ 2.2 <sup>***</sup>

Cell viability was measured as MTT reduction and data were normalized as % control. Data are expressed as the means  $\pm$  SEM in triplicate of at least three different cultures. All compounds were assayed at increasing concentrations (1–300  $\mu\text{M}$ ). <sup>\*\*\*</sup> $P \leq 0.001$ , <sup>\*\*</sup> $P \leq 0.01$ , <sup>\*</sup> $P \leq 0.05$  and <sup>ns</sup>not significant, with respect to the control group. Comparisons between drugs and the control group were performed by one-way ANOVA followed by the Newman–Keuls post-hoc test.

## Notes and references

- 1 L. Wang, W.-J. Lu, T. Odawara, R. Misumi, Z.-W. Mei, W. Peng, I. E.-T. El-Sayed and T. Inokuchi, *J. Heterocycl. Chem.*, 2014, **51**, 1106–1114.
- 2 Z.-W. Mei, L. Wang, W.-J. Lu, C.-Q. Pang, T. Maeda, W. Peng, M. Kaiser, I. El Sayed and T. Inokuchi, *J. Med. Chem.*, 2013, **56**, 1431–1442.
- 3 R. León, A. G. García and J. Marco-Contelles, *Med. Res. Rev.*, 2013, **33**, 139–189.
- 4 A. Samadi, C. Valderas, C. de los Ríos, A. Bastida, M. Chioua, L. González-Lafuente, L. Colmena, I. Gandía, A. Romero, L. del Barrio, M. D. Martín-de-Saavedra, M. G. López, M. Villarroya and J. Marco-Contelles, *Bioorg. Med. Chem.*, 2011, **19**, 122–133.
- 5 H. W. Querfurth and F. M. LaFerla, *N. Engl. J. Med.*, 2010, **362**, 329–344.
- 6 D. J. Selkoe, *Physiol. Rev.*, 2001, **81**, 741–766.
- 7 P. R. Bosboom, H. Alfonso, J. Eaton and O. P. Almeida, *Int. Psychogeriatr.*, 2012, **24**, 708–721.
- 8 P. A. Adlard, S. A. James, A. I. Bush and C. L. Masters, *Drugs Today*, 2009, **45**, 293–304.
- 9 P. T. Francis, A. M. Palmer, M. Snape and G. K. Wilcock, *J. Neurol., Neurosurg. Psychiatry*, 1999, **66**, 137–147.
- 10 N. C. Danbolt, *Prog. Neurobiol.*, 2001, **65**, 1–105.
- 11 F. Massoud and S. Gauthier, *Curr. Neuropharmacol.*, 2010, **8**, 69–80.
- 12 L. A. Craig, N. S. Hong and R. J. McDonald, *Neurosci. Biobehav. Rev.*, 2011, **35**, 1397–1409.
- 13 C. G. Ballard, *Eur. Neurol.*, 2002, **47**, 64–70.
- 14 F. Zemek, L. Drtinova, E. Nepovimova, V. Sepsova, J. Korabecny, J. Klimes and K. Kuca, *Expert Opin. Drug Saf.*, 2014, **13**, 759–774.
- 15 U. Holzgrabe, P. Kapková, V. Alptüzün, J. Scheiber and E. Kugelmann, *Expert Opin. Ther. Targets*, 2007, **11**, 161–179.
- 16 K. L. Davis and P. Pochwik, *Lancet*, 1995, **11**, 625–630.
- 17 V. Tumiatti, A. Minarini, M. L. Bolognesi, A. Milelli, M. Rosini and C. Melchiorre, *Curr. Med. Chem.*, 2010, **17**, 1825–1838.
- 18 M. H. M. Sharaf, P. L. Schiff, A. N. Tackie, C. H. Phoebe and G. E. Martin, *J. Heterocycl. Chem.*, 1996, **33**, 239–243.
- 19 A. Paulo, E. T. Gomes, J. Steele, D. C. Warhurst and P. J. Houghton, *Planta Med.*, 2000, **66**, 30–34.
- 20 D. M. Du and P. R. Carlier, *Curr. Pharm. Des.*, 2004, **10**, 3141–3156.
- 21 D. Muñoz-Torrero and P. Camps, *Curr. Med. Chem.*, 2006, **13**, 399–422.
- 22 Y. P. Pang, P. Quiram, T. Jelacic, F. Hong and S. Brimijoin, *J. Biol. Chem.*, 1996, **271**, 23646–23649.
- 23 A. Romero, R. Cacabelos, M. J. Oset-Gasque, A. Samadi and J. Marco-Contelles, *Bioorg. Med. Chem. Lett.*, 2013, **23**, 1916–1922.
- 24 J.-S. Lan, S.-S. Xie, S.-Y. Li, L.-F. Pan, X.-B. Wang and L.-Y. Kong, *Bioorg. Med. Chem.*, 2014, **22**, 6089–6104.
- 25 P. R. Carlier, D.-M. Du, Y. Han, J. Liu and Y.-P. Pang, *Bioorg. Med. Chem. Lett.*, 1999, **9**, 2335–2338.
- 26 L. Wang, M. Switalska, Z.-W. Mei, W.-J. Lu, Y. Takahara, X.-W. Feng, I. E.-T. El-Sayed, J. Wietrzyk and T. Inokuchi, *Bioorg. Med. Chem.*, 2012, **20**, 4820–4829.
- 27 G. L. Ellman, K. D. Courtney, V. Andres Jr. and R. M. Feather-Stone, *Biochem. Pharmacol.*, 1961, **7**, 88–95.
- 28 M. L. Bolognesi, A. Cavalli, L. Valgimigli, M. Bartolini, M. Rosini, V. Andrisano, M. Recanatini and C. Melchiorre, *J. Med. Chem.*, 2007, **50**, 6446–6449.
- 29 X. Zha, D. Lamba, L. Zhang, Y. Lou, C. Xu, D. Kang, L. Chen, Y. Xu, L. Zhang, A. De Simone, S. Samez, A. Pesaresi, J. Stojan, M. G. López, J. Egea, V. Andrisano and M. Bartolini, *J. Med. Chem.*, 2016, **59**, 114–131.
- 30 E. Nepovimova, E. Uliassi, J. Korabecny, L. E. Pena-Altamira, S. Samez, A. Pesaresi, G. E. García, M. Bartolini, V. Andrisano, C. Bergamini, R. Fato, D. Lamba, M. Roberti, K. Kuca, B. Monti and M. L. Bolognesi, *J. Med. Chem.*, 2014, **57**, 8576–8589.
- 31 S. Butini, M. Brindisi, S. Brogi, S. Maramai, E. Guarino, A. Panico, A. Saxena, V. Chauhan, R. Colombo, L. Verga, E. De Lorenzi, M. Bartolini, V. Andrisano, E. Novellino, G. Campiani and S. Gemma, *ACS Med. Chem. Lett.*, 2013, **4**, 1178–1182.
- 32 C. Galdeano, E. Viayna, I. Sola, X. Formosa, P. Camps, A. Badía, M. V. Clos, J. Relat, M. Ratia, M. Bartolini, F. Mancini, V. Andrisano, M. Salmona, C. Minguillon, G. C. González-Muñoz, M. I. Rodríguez-Franco, A. Bidon-Chanal, F. J. Luque and D. Muñoz-Torrero, *J. Med. Chem.*, 2012, **55**, 661–669.
- 33 S. Rizzo, A. Bisi, M. Bartolini, F. Mancini, F. Belluti, S. Gobbi, V. Andrisano and A. Rampa, *Eur. J. Med. Chem.*, 2011, **46**, 4336–4343.
- 34 C. Ronco, E. Carletti, J.-Ph. Colletier, M. Weik, F. Nachon, L. Jean and P.-Y. Renard, *ChemMedChem*, 2012, **7**, 400–405.
- 35 M. I. Rodríguez-Franco, M. I. Fernández-Bachiller, C. Pérez, B. Hernández-Ledesma and B. Bartolomé, *J. Med. Chem.*, 2006, **49**, 459–462.
- 36 S. Butini, G. Campiani, M. Borriello, S. Gemma, A. Panico, M. Persico, B. Catalanotti, S. Ros, M. Brindisi, M. Agnusdei, I. Fiorini, V. Nacci, E. Novellino, T. Belinskaya, A. Saxena and C. Fattorusso, *J. Med. Chem.*, 2008, **51**, 3154–3170.
- 37 O. Trott and A. J. Olson, *J. Comput. Chem.*, 2010, **31**, 455–461.
- 38 M. Bartolini, M. Pistolozzi, V. Andrisano, J. Egea, M. G. López, I. Iriepa, I. Moraleda, E. Gálvez, J. Marco-Contelles and A. Samadi, *ChemMedChem*, 2011, **6**, 1990–1997.
- 39 A similar analysis has been carried to investigate the docking of compound 1-3 on hBuChE (ESI†).
- 40 A. Minarini, A. Milelli, V. Tumiatti, M. Rosini, E. Simoni, M. L. Bolognesi, V. Andrisano, M. Bartolini, E. Motori, C. Angeloni and S. Hrelia, *Neuropharmacology*, 2012, **62**, 997–1003.
- 41 S. Brogi, S. Butini, S. Maramai, R. Colombo, L. Verga, C. Lanni, E. De Lorenzi, S. Lamponi, M. Andreassi, M. Bartolini, V. Andrisano, E. Novellino, G. Campiani, M. Brindisi and S. Gemma, *CNS Neurosci. Ther.*, 2014, **20**, 624–632.

- 42 A. A. Reinke and J. E. Gestwicki, *Chem. Biol. Drug Des.*, 2007, **70**, 206–215.
- 43 M. Bartolini, C. Bertucci, M. L. Bolognesi, A. Cavalli, C. Melchiorre and V. Andrisano, *ChemBioChem*, 2007, **8**, 2152–2161.
- 44 M. Citron, *Nat. Rev. Drug Discovery*, 2010, **9**, 387–398.
- 45 D. Schlenzig, S. Manhart, Y. Cinar, M. Kleinschmidt, G. Hause, D. Willbold, S. A. Funke, S. Schilling and H. U. Demuth, *Biochemistry*, 2009, **48**, 7072–7078.
- 46 F. Denizot and R. Lang, *J. Immunol. Methods*, 1986, **89**, 271–277.